Army Research Laboratory

Magnetic Modeling of a Rotating Flux Concentrator System Designed to Mitigate Noise in "Large" Magnetic Sensors

by Gregory A. Fischer and Alan S. Edelstein

ARL-TR-5317 **September 2010**

NOTICES

Disclaimers

The findings in this report are not to be construed as an official Department of the Army position unless so designated by other authorized documents.

Citation of manufacturer's or trade names does not constitute an official endorsement or approval of the use thereof.

Destroy this report when it is no longer needed. Do not return it to the originator.

Army Research Laboratory

Adelphi, MD 20783-1197

ARL-TR-5317 **September 2010**

Magnetic Modeling of a Rotating Flux Concentrator System Designed to Mitigate Noise in "Large" Magnetic Sensors

Gregory A. Fischer and Alan S. Edelstein
Sensors and Electron Devices Directorate, ARL

REPORT DOCUMENTATION PAGE

Form Approved
OMB No. 0704-0188

1. REPORT DATE *(DD-MM-YYYY)* September 2010	**2. REPORT TYPE** Final	**3. DATES COVERED (From - To)** May 2009 to July 2010

4. TITLE AND SUBTITLE

Magnetic Modeling of a Rotating Flux Concentrator System Designed to Mitigate Noise in “Large” Magnetic Sensors

5a. CONTRACT NUMBER

5b. GRANT NUMBER

5c. PROGRAM ELEMENT NUMBER

6. AUTHOR(S)

Gregory A. Fischer and Alan S. Edelstein

5d. PROJECT NUMBER

5e. TASK NUMBER

5f. WORK UNIT NUMBER

7. PERFORMING ORGANIZATION NAME(S) AND ADDRESS(ES)

U.S. Army Research Laboratory
ATTN: RDRL-SES-P
2800 Powder Mill Road
Adelphi, MD 20783-1197

8. PERFORMING ORGANIZATION REPORT NUMBER

ARL-TR-5317

9. SPONSORING/MONITORING AGENCY NAME(S) AND ADDRESS(ES)

DARPA
3701 Fairfax Dr
Arlington VA 22203

10. SPONSOR/MONITOR’S ACRONYM(S)

11. SPONSOR/MONITOR'S REPORT NUMBER(S)

12. DISTRIBUTION/AVAILABILITY STATEMENT

Approved for public release; distribution unlimited.

13. SUPPLEMENTARY NOTES

14. ABSTRACT

This report discusses the magnetic modeling results of a proof of concept system for 1/*f* noise mitigation in “large” sensors. The 1/*f* noise reduction is achieved by rotating flux concentrators that shift the operating frequency of the sensor to higher frequencies where 1/*f* noise is lower. The goal is to design systems with magnetic flux concentrators that maximize the enhancement of the field and the percentage modulation of the field but minimize size. These issues in execution and necessary tradeoffs in performance are discussed, and magnetic modeling is presented, showing a clear road map to increased performance from the viewpoint of field enhancement and modulation.

15. SUBJECT TERMS

Magnetic modeling, 1/*f* noise, magnetic sensors, flux concentrator

16. SECURITY CLASSIFICATION OF:			**17. LIMITATION OF ABSTRACT**	**18. NUMBER OF PAGES**	**19a. NAME OF RESPONSIBLE PERSON** Gregory A. Fischer
a. REPORT Unclassified	**b. ABSTRACT** Unclassified	**c. THIS PAGE** Unclassified	UU	22	**19b. TELEPHONE NUMBER** (*Include area code*) (301) 394-2089

Standard Form 298 (Rev. 8/98)
Prescribed by ANSI Std. Z39.18

Contents

List of Figures

List of Tables

Acknowledgments

This work was supported by the Defense Advanced Research Projects Agency (DARPA) under the Heterostructural Uncooled Magnetic Sensor (HUMS) Program.

Executive Summary

There are numerous applications that can benefit from small, inexpensive, low-power, low-frequency sensors capable of detecting ultra-low magnetic fields not only within the military community but also in the areas of medical diagnostics, information technology, and commercial industry (*1*). Until recently, the detection of fields between 1 pT (10^{-8} Oe) and 0.1 nT (10^{-6} Oe) was dominated by relatively large, expensive, power-hungry sensors such as fluxgates, optically pumped magnetometers, and superconducting quantum interference devices (SQUIDs). Advances in magnetic tunnel junctions MgO barriers combined with concepts for mitigating the 1/*f* noise present in these magnetoresistive devices open the possibility of using small, low-power, high-sensitivity devices for the detection of weak, low frequency magnetic fields (*2–4*). Extending magnetic sensor sensitivity to the sub-picotesla range necessitates looking beyond just the limitations imposed by 1/*f* noise. It can be shown (*5*) that by increasing the volume of the sensor or the sensing element area from microns to 1 or 2 cm^2, an additional gain in sensitivity can be achieved. Magnetoresistive sensors are intrinsically small. In contrast to magnetoresistance sensors, magnetoelectric sensors are inherently larger sensors because their output signal increases with their length. Magnetoelectric sensing elements can be made in the appropriate size range such that, with the mitigation of 1/*f* noise, sub-picotesla sensitivity is possible.

This report presents magnetic modeling results of a proof of concept system for 1/*f* noise mitigation in “large” sensors. The 1/*f* noise reduction is achieved by rotating flux concentrators that shift the operating frequency of the sensor to higher frequencies where 1/*f* noise is lower. The goal is to design systems with magnetic flux concentrators that maximize the enhancement of the field and the percentage modulation of the field but minimize size. These issues in execution and necessary tradeoffs in performance are discussed, and magnetic modeling is presented, showing a clear road map to increased performance from the viewpoint of field enhancement and modulation. In order for the magnetoelectric sensor team to meet the metrics of the Defense Advanced Research Projects Agency (DARPA) Heterostructural Uncooled Magnetic Sensor (HUMS) Program, it is essential that a solution be found.

INTENTIONALLY LEFT BLANK.

1. Introduction

Considerable progress has been made recently in magnetic sensors, including (1) the discovery (*4, 6*) that using MgO barriers in magnetic tunnel junctions leads to magnetoresistance values as large as several hundred percent and (2) the invention (*7*) of magnetoelectric sensors. Magnetoelectric sensors are composed of a piezoelectric material sandwiched between slabs of a magnetostrictive material. In a magnetic field the magnetostrictive material stresses the piezoelectric material which, in turn, generates a voltage. Thus, an output is generated without using any input power. These magnetoelectric sensors already have a sensitivity of less than 1 nT and they must have dimensions of several centimeters to maintain good sensitivity.

The sensitivity of magnetic sensors is limited by the magnitude of their response to a magnetic field and their noise. Sensors with larger responses to a magnetic field also tend to have larger $1/f$ noise. Figure 1 shows an example to $1/f$ noise in an electromechanical sensor. Because of the importance of $1/f$ noise, anisotropic magnetic sensors that only have magnetoresistance values of less than 3.5% are still widely used because their $1/f$ noise is small. The large $1/f$ noise in magnetic tunnel junctions with MgO barriers has limited their use at low frequencies. This led to research (*8*) on the micro-electromechanical system (MEMS) flux concentrator, a device that modulates the field and thus increases the modulation frequency to a region where $1/f$ noise is less important. The MEMS flux concentrator is a viable solution for solving the problem of $1/f$ noise in small magnetic sensors.

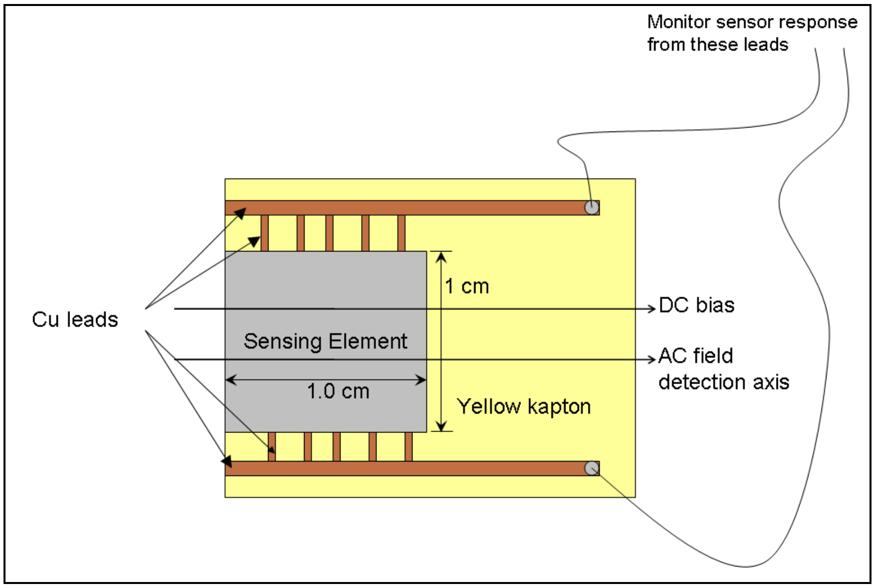

Figure 1. Schematic of magnetoelectric sensor. The gray region consists of a piezoelectric material sandwiched between slabs of a magnetostrictive material. Sensitivity is already under 1 nT.

Besides the 1/*f* noise term, there are other contributions to the noise. Both shot noise and thermal magnetic noise (*5*), which depend on the size of the sensor, are important. Thus, to achieve sub-pT sensitivities it is probably necessary to use larger sensors. These points make magnetoelectric sensing elements excellent candidates. Since the MEMS flux concentrator was designed to be used with small sensors, a different approach is needed to achieve sub-pT sensitivities with large magnetic sensors. We describe a new approach, based on using a rotating disk, which allows us to modulate the field for sensors occupying a volume of about 1 cubic cm. An essential part of designing the device was understanding the behavior of the magnetic field lines both for enhancing the field at the position of the sensor as well as maximizing modulation of the field. These needs motivated the work on macro-magnetic modeling described in this report.

2. Magnetic Modeling Details and Parameters

We performed magnetic modeling using a commercial finite element code program called Maxwell 3D, from ANSYS. Maxwell 3D is capable of analyzing AC magnetic, DC magnetic, and electrostatic field problems. The 3D DC magnetic portion of the software computes static magnetic fields where the source originates from a DC current or voltage, permanent magnets, or externally applied magnetic fields. It can directly compute the magnetic field (H) and current distribution (J), and derive the magnetic flux density (B) from the H field. In addition, it can automatically calculate force, torque, inductances, and saturation in devices containing linear, nonlinear, and anisotropic materials. The post-processor portion of the software can provide plots of flux lines, B and H fields, energy densities, and saturation. The modeling process consists of drawing the objects of interest, assigning properties (coercivity, permeability, etc.) to the objects, assigning boundaries or sources, seeding the objects and creating a mesh, and then processing the now defined problem.

Each model investigated involved the same fundamental sequence of steps. The first step in the analysis of the flux concentrator was to draw the model. Drawing the model consists of drawing three dimensional objects and either joining them together or subtracting them from each other. This allows one to create complex objects. A sufficiently large region around the flux concentrators and the sensing region were defined as a background. The flux concentrators were drawn as solid pieces and assigned the material properties of permalloy (NiFe), with a permeability of 5000 as that is a value readily achieved in this material. The material properties assigned to this background are those of a vacuum, with a relative permeability of 1. The modeling is macro-magnetic in nature, as it does not take into account domain structure but does incorporate demagnetization factors. The initial mesh is created by the program, but one can create regions in which the initial mesh is denser so as to force more tetrahedrons into regions where one has a greater interest in the solutions without significantly increasing solution time.

Mesh refinement is also handled by the program as part of an iterative process in which energy error and percentage decrease to a predetermined figure. All nonmagnetic structural material was ignored. The magnetic material of the sensor was also ignored as the thicknesses of the various layers are small enough to have only a small influence on the surrounding flux environment.

We are interested in the magnetic field strength and flux line behavior at the position the sensor would occupy. Two main quantities of interest to us are the enhancement factor and the percentage modulation. The enhancement factor is defined as H_S/H_{appl}, where H_S and H_{appl} denote the magnetic field strength at the position of the sensor and the applied magnetic field strength, respectively. For the rotating flux concentrator design, there are two main positions to consider: (1) the position in which the magnetic field is at a maximum value at the sensor location and (2) the position that achieves a minimum in field strength, or shunts the field away, at the sensor position. Periodic motion between these two positions at a high frequency modulates the field, thus achieving the desired shift of the operating frequency of the sensor to higher frequencies where 1/*f* noise is lower. We then define the percentage field modulation at the position of the sensor as

$$E_H(max)/ E_H(min) * 100 \tag{1}$$

where $E_H(max)$ and $E_H(min)$ are the enhancement factors at the maximum and minimum magnetic field strength positions, respectively. Section 3 discusses the designs we have modeled.

3. Rotating Flux Concentrator Designs

Due to the size of the sensor (figure 1), we decided that the best way to modulate the field was via rotation. The first design to be discussed was modeled but never constructed. Designs 2 and 3 were both modeled and constructed.

3.1 Magnetic Modeling Results for Design 1

This design is essentially a compound flux concentrator system. There are two pairs of concentric flux concentrators in close proximity to each other. As shown in figure 2, the inner most pair of concentrators is stationary while the outermost pair rotates around the common center axis. The sensor position would be at the origin of the shown coordinate axis. The parameters that were varied for this design were (1) the permalloy thickness of the concentrators and (2) the length of the rotating concentrators. The air gap between the innermost pair of concentrators, the region which would contain the sensor, was set to 1.5 mm and the air gap between the stationary and rotating concentrators was set to 0.1 mm (figure 3). An initial model indicated that a deposition of a thin layer of permalloy, 0.25 microns, would only result in a maximum enhancement value of 1.2. Subsequent models used a permalloy thickness of 0.2 mm.

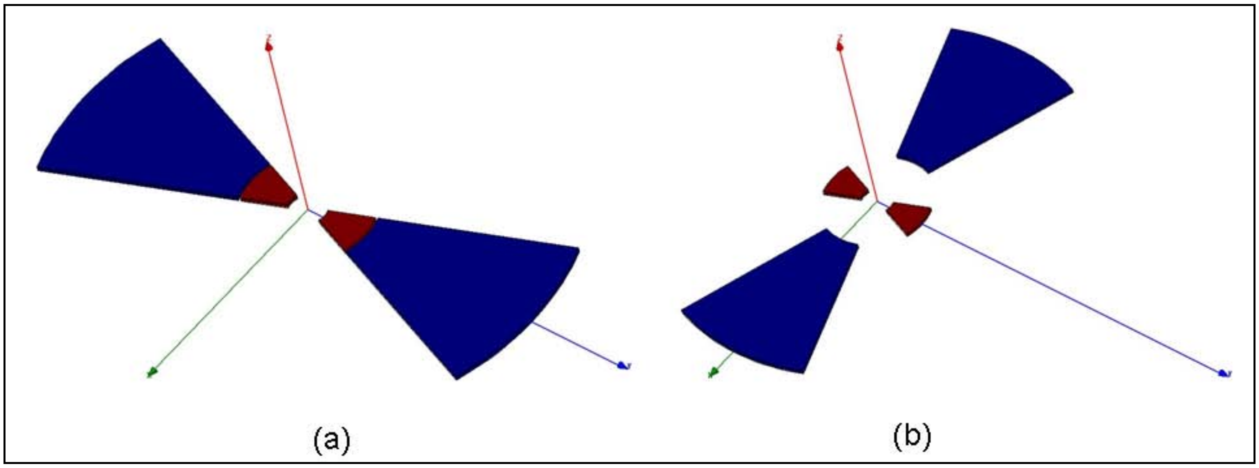

Figure 2. First concept of rotating flux concentrators. The red concentrators are stationary and the blue concentrators are free to rotate. The maximum magnetic field enhancement at the origin of the coordinate axis is achieved when (a) the concentrators are aligned and the minimum is achieved when (b) the outermost pair of concentrators have rotated 90° from the position shown in (a).

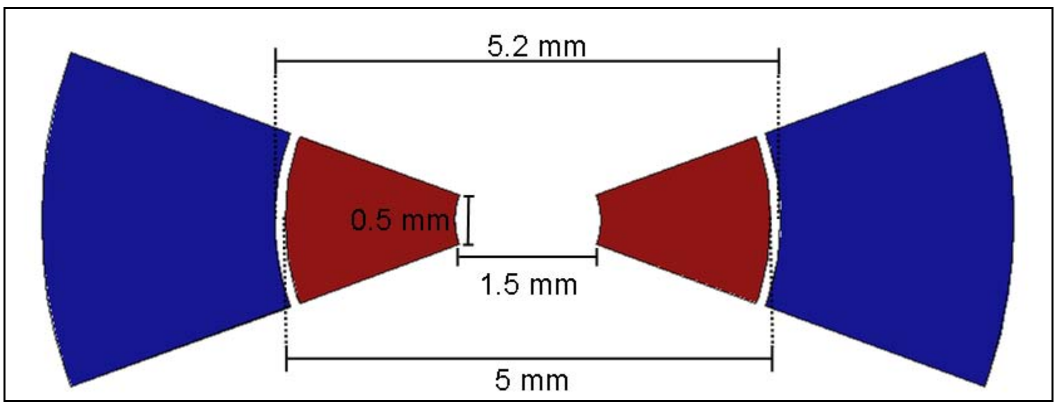

Figure 3. Schematic of design 1 showing various dimensions of interest.

With the permalloy thickness now held constant, we ran the first model with the length of the stationary magnetic flux concentrators set to 7.4 mm. The maximum field enhancement achieved for this model was 2.15. In an effort to increase this enhancement value, we next increased the length of the rotating concentrators to 17.4 mm. As we see in figure 4, the aligned flux concentrators do a good job of focusing the magnetic flux lines at the origin of the coordinate axis and the maximum enhancement value was determined to be 3.46. However, knowing that (1) the air gap was already smaller than the electromagnetic sensor we would eventually use, (2) it would be difficult to run electrical leads to a sensor at the center of rotation, and (3) the 0.1 mm gap between the inner and outer flux concentrators is a challenge given the high speed of rotation that would required of the inner concentrators, we decided to alter the design.

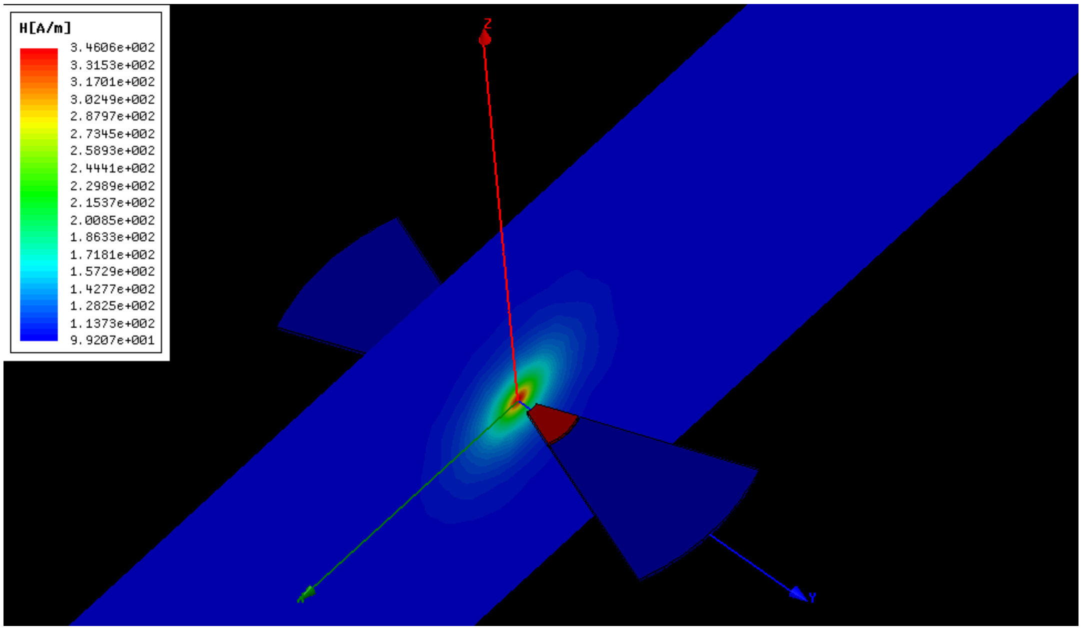

Figure 4. Plot of the magnetic field strength in the plane perpendicular to the *x*-*y* plane for the position producing a maximum value of enhancement at the origin.

3.2 Magnetic Modeling Results for Design 2

The initial design is shown in figure 5. The sensor is positioned about 1 mm above and centered on the edge of the rotating disc. The rotation is driven by an electrical motor and the rotation rate is monitored by using a photo cell and holes in the disc. Thin pieces (0.25 mm thick) of sheet permalloy on the disc act either as flux concentrators or as flux shunts that shield the sensor from the magnetic flux.

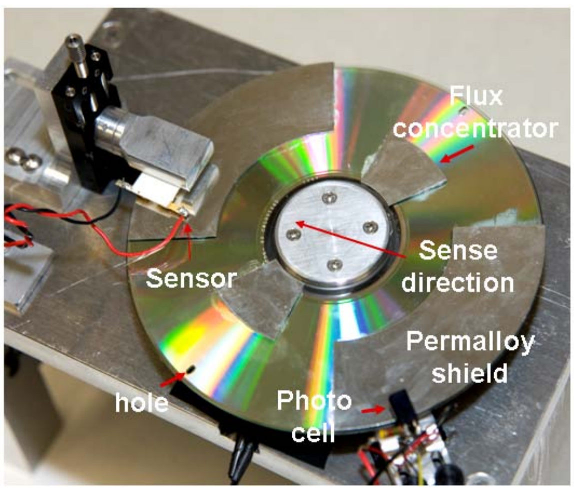

Figure 5. Rotating flux concentrator apparatus.

The results of modeling the flux concentrator apparatus are shown for two orientations in figure 6. Extracting the data from the models to determine the enhancement factors lead to a startling result. The enhancement factor for the "shunt" position (figure 6b) is 1.02 and, for the "concentrating" position (figure 6a), it is 0.45. While this leads to a modulation percentage of about 225%, it was clear the design was not influencing the flux lines as we had envisioned.

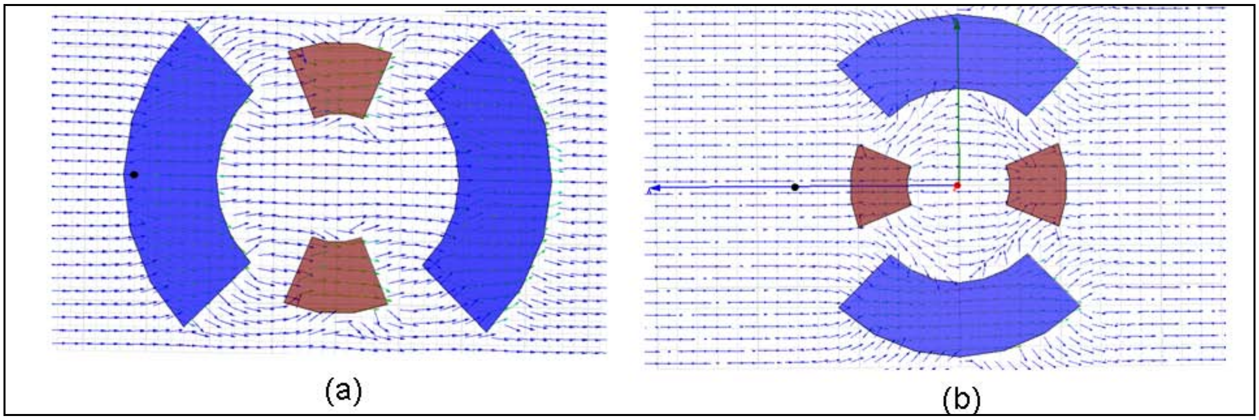

Figure 6. Model results showing the magnetic field lines for (a) the "shunt" and (b) the "concentration" orientation. The sensor position is indicated by the black dot. Permalloy shunts are shown in blue and the concentrators in red. Large arrows in (b) are the reference axis directions.

Plotting the enhancement factors for several orientations of the disc produces a modulation curve and serves to illustrate that the shunt position actually maximizes the field strength at the position of the sensor as the disc rotates (figure 7). We had initially believed that the permalloy shields below the sensor would pull the magnetic field away from the sensor location and allow the field lines to circulate around the center of the disc while the concentrators would provide more of a direct line path for flux lines, thus enhancing the field at the position of the sensor. Figure 6 supports this line of reasoning; however, if we look at the magnetic flux lines out of the plane of the rotating disc (figure 8), we see that because the permalloy shields extend all the way out to the edge, the magnetic flux lines curl down into the shields *through* the sensor position. This results in the magnetic field strength actually being higher at the sensor location in the shunt position.

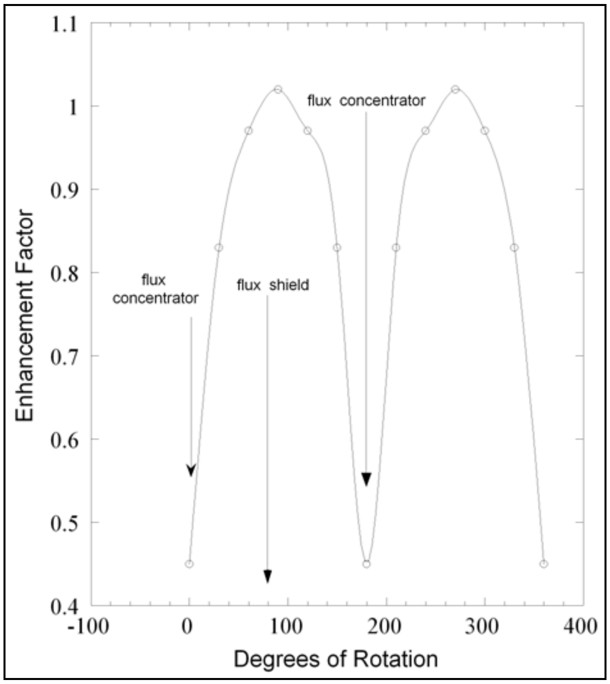

Figure 7. Modulation curve for design 2.

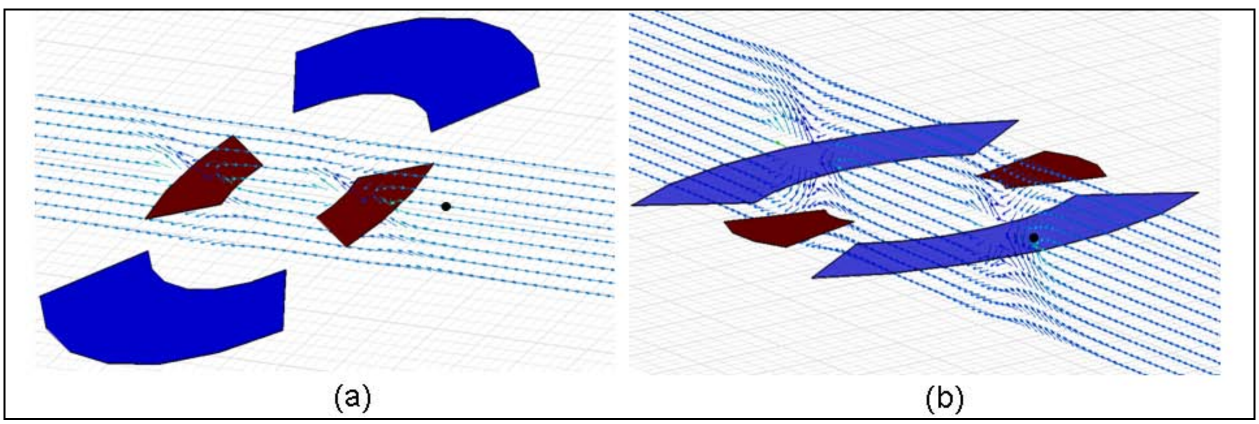

Figure 8. Magnetic field lines in a plane perpendicular to the concentrators for (a) the "concentration" orientation and (b) the "shunt" position. Sensor position is indicated by the black dot. Note the flux lines curling down through the sensor location in (b).

3.3 Magnetic Modeling Results for Design 3

While the modulation percentage of our second design was adequate, the enhancement factor for concentrating the field at the position of the sensor needed to be higher. The new design we considered is shown in figure 9. The permalloy shunts and concentrators have been replaced with a single strip of permalloy, 0.25 mm thick and 40 mm wide, running across the diameter of the disc and cut to conform to the curvature of the disc's edge. Additionally, two permalloy rods have been added to the apparatus. These rods were heat treated to maximize their magnetic permeability after they had been cut and machined. This new design also uses a non-ferrous air turbine to spin the disc. This was done because the electric motor of design 2 was raising the noise floor, creating extra peaks, and broadening other peaks in the frequency domain (figure 10).

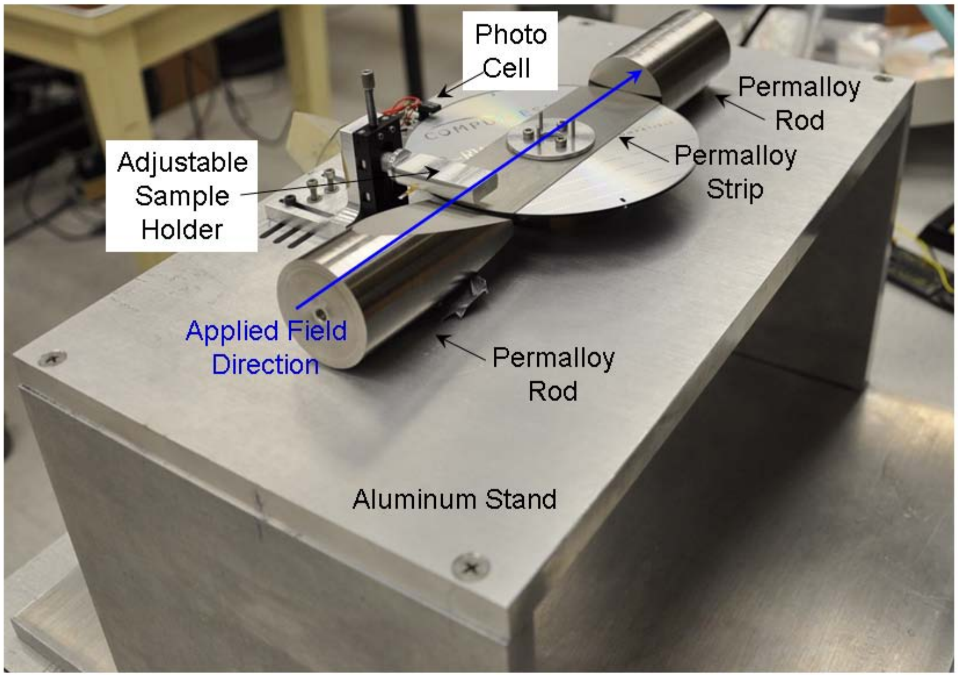

Figure 9. Design 3 of the rotating flux concentrator, showing all of the essential elements except for brackets to hold the permalloy rods in place and the non-ferrous air turbine designed to spin the disc.

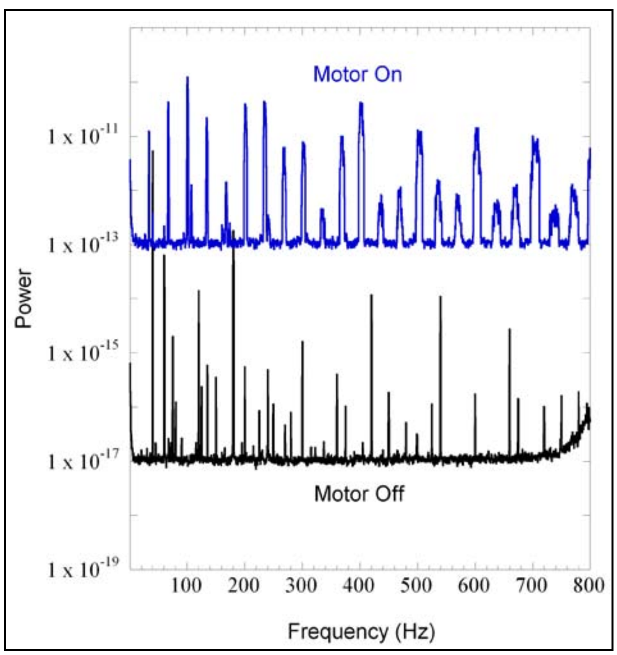

Figure 10. Comparison of the noise with a stationary disc and with the disc being rotated by an electric motor.

We ran several models to ascertain the optimum combination of sensor height above the disc as well as air gap size between the permalloy rods and the disc. Here we present the magnetic modeling results for the optimized design parameters. For this design, the sensor is centered on, and 2 mm above, the edge of the disc. The permalloy rod on the side away from the sensor is 3 mm away from, and centered on, the edge the disc, and the beveled permalloy rod near the sensor is 6 mm away from, and centered on, the edge of the disc. Figure 11 shows the dimensions of the beveled disc and figure 12 shows the sensor position relative to the rod. The enhancement factor for the “concentrating” position (figure 13a) is 8.36 and, for the “shunting position” position (figure 13b), it is 2.67. This leads to a modulation percentage of about 313% at the position of the sensor.

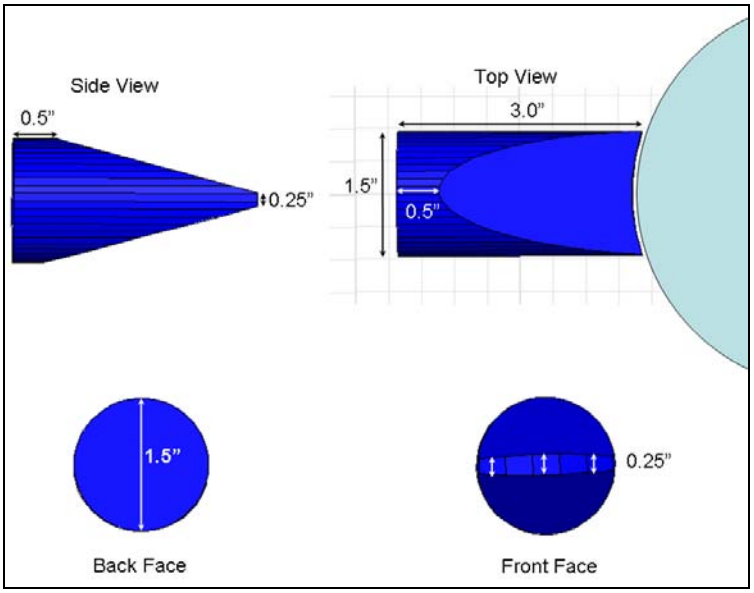

Figure 11. Dimensions of the beveled permalloy rod.

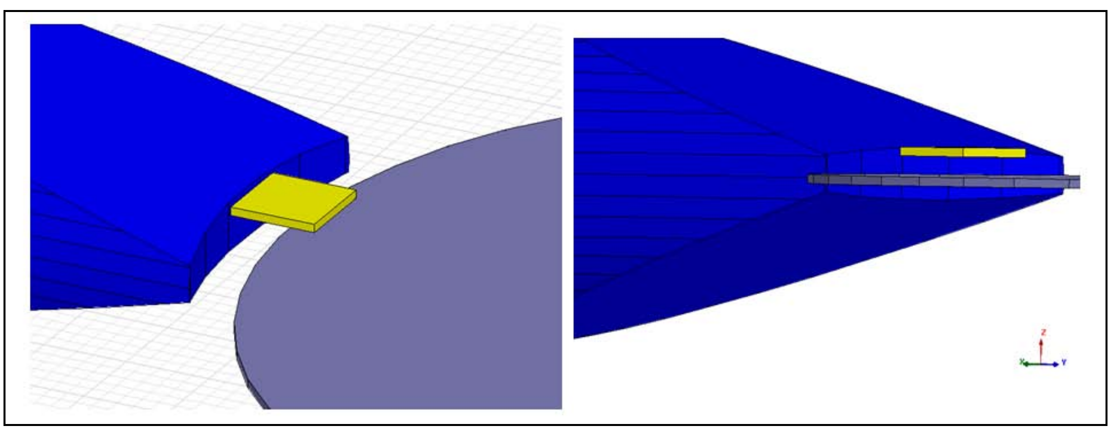

Figure 12. Magnetoelectric sensor position relative to the beveled rod and disc. The sensor is shown in yellow.

Examination of figure 13 indicates that in the “concentration” position field lines are being focused through the sensor position toward the permalloy strip. In the shunt position, the magnetic field lines are less focused and are curling away from the sensor position. While the enhancement factor is higher in the shunt position for this design than in design 2, the maximum enhancement is now 8× higher, thus providing a greater degree of field enhancement as well as increasing the modulation at the sensor location.

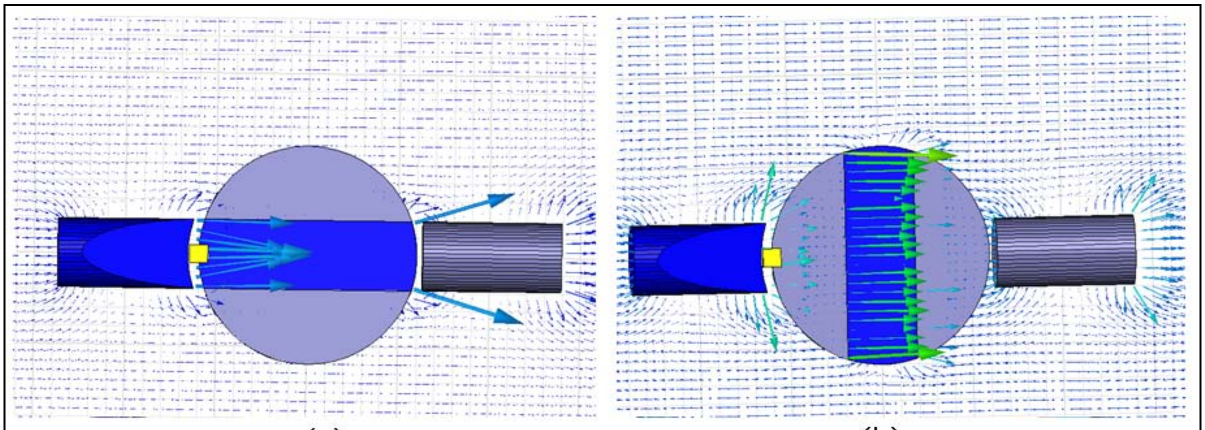

Figure 13. Model results showing the magnetic field lines for the (a) “concentration” and (b) “shunt” orientation. The sensor position is indicated by the yellow square. Permalloy strip and beveled rod are shown in blue while the flat-faced rod is shown in gray. The magnetic field strength is denoted by color and size of the arrows, with small and dark blue being low, and large and green being high.

4. Conclusion

We have shown how magnetic modeling helped to design a device that mitigates 1/*f* noise in large magnetic field sensors. The results are summarized in table 1. Focusing on the key design elements of air gaps, sensor position, and the arrangement of pieces of permalloy to serve as flux concentrators and shunts, we were able to create a design, which, when used with magnetoelectric sensors, should yield both a field enhancement and modulation sufficient to achieve less than 1 $pT/Hz^{1/2}$ at 1 Hz detectivity.

Table 1. Summary of enhancement factors and percentage modulation at the position of the sensor.

	E_H(max)	E_H(min)	Percentage Modulation
Design 1	3.46	n/a	n/a
Design 2	1.02	0.45	225
Design 3	8.36	2.67	313

5. References

1. Lenz, J.; Edelstein, A. Magnetic Sensors and Their Applications. *IEEE Sensors* **June 2006**, *6*, 631–49.

2. Edelstein, A. S.; Burnette, J.; Fischer, G. A.; Cheng, S. F.; Egelhoff, W. F., Jr.; Pong, P.W.T.; McMichael, R. D. Advances in Magnetometry Through Miniaturization. *J. Vac. Sci. Technol. A* **July 2008**, *26*, 757–62.

3. Guedes, A.; Patil, S. B.; Wisniowski, P.; Chu, V.; Conde, J. P.; Freitas, P. P. Hybrid Magnetic Tunnel Junction-MEMS High Frequency Field Modulator for 1/f Noise Suppression. *IEEE Trans. Magn.* **November 2008**, *44*, 2554–7.

4. Parkin, S.S.P.; Kaiser, C.; Panchula, A.; Rice, P. M.; Hughs, B.; Samant M.; Yang, S. Giant Tunneling Magnetoresistance at Room Temperature with MgO (110) Tunnel Barriers. *Nat. Mater*. **December 2004**, *3*, 862–7.

5. Egelhoff, W. F., Jr.; Pong, P.W.T.; Unguris, J.; McMichael, R. D.; Nowak, E. R.; Edelstein, A. S.; Burnette, J. E. Fisher, G. A. Critical Challenges for picoTesla Magnetic-tunnel-junction Sensors. *Sens. Actuators A* **October 2009**, *155*, 217–25.

6. Butler, W. H.; Zhang, X.-G.; Schulthess, T. C.; MacLaren, J. M. Spin-dependent Tunneling Conductance of Fe|MgO|Fe Sandwiches. *Phys. Rev B* **2001**, *63*, 054416/1–12.

7. Das, J.; Li, M.; Kalarickal, S. S.; Altmannshofer, S.; Buchanan, K. S.; Li, J. F.; Viehland, D. Control of Magnetic and Electric Responses with Electric and Magnetic Fields in Magnetoelectric Heterostructures. *Appl. Phys. Lett.* **2010**, *96*, 222508.

8. Edelstein, A. S.; Burnette, J. E.; Fischer, G. A.; Olver, K.; Eglehoff, Wm.; Nowak, E.; Cheng, Shu-Fan. Validation of the Microelectromechanical System Flux Concentrator Concept for Minimizing the Effect of 1/*f* Noise. *J. Appl. Phys.* **2009**, *105*, 07E720, 2009.

NO. OF COPIES	ORGANIZATION
1 ELEC	ADMNSTR DEFNS TECHL INFO CTR ATTN DTIC OCP 8725 JOHN J KINGMAN RD STE 0944 FT BELVOIR VA 22060-6218
1	DEFNS INTLLGNC AGCY ATTN RTS-2A TECHL LIB WASHINGTON DC 20301
1	US ARDEC ATTN AMSRD AAR HEP A M HOHIL BLDG 407 PICATINNY ARSENAL NJ 07806-5000
1	US ARMY ARDEC ATTN AMSRD AAR AEP S R T KINASEWITZ BLDG 353N PICATINNY ARSENAL NJ 07806-5000
1	US ARMY ARDEC ATTN AMSRD AAR EMK TECH LIB BLDG 59 PHIPPS RD PICATINNY ARSENAL NJ 07806-5000
1	NAV RSRCH LAB ATTN 5220 TECHL LIB 4555 OVERLOOK AVE SW WASHINGTON DC 20375-5320
1	THE JOHNS HOPKINS UNIV APPLD PHYSIC LAB ATTN TECH LIB JOHNS HOPKINS RD LAUREL MD 20707
1	SOUTHWEST RSRCH INST ATTN S CERWIN 6220 CALEBRA RD SAN ANTONIO TX 78238

NO. OF COPIES	ORGANIZATION
2	SSP ATTN C GILBREATH, ASSOC TECH DIR ATTN T HAWLEY TECHL DIR 11781 LEE JACKSON MEMORIAL HWY FAIRFAX VA 22033-3309
1	US ARMY RSRCH LAB ATTN RDRL CIM G T LANDFRIED BLDG 4600 ABERDEEN PROVING GROUND MD 21005-5066
18	US ARMY RSRCH LAB ATTN IMNE ALC HRR MAIL & RECORDS MGMT ATTN RDRL CIM L TECHL LIB ATTN RDRL CIM P TECHL PUB ATTN RDRL SE J PELLEGRINO ATTN RDRL SES J EICKE ATTN RDRL SES P A EDELSTEIN ATTN RDRL SES P G FISCHER (10 COPIES) ATTN RDRL SES P J FINE ATTN RDRL SES P M SCANLON ADELPHI MD 20783-1197

TOTAL: 29 (28 HCS, 1 ELEC)